Two different incorporation sites of manganese in single-crystalline monohydrated *L*-asparagine studied by electron paramagnetic resonance

K. Krambrock, K. J. Guedes, and L. O. Ladeira
Departamento de Física, ICEx, Universidade Federal de Minas Gerais, Caixa Postal 702, 30123 Belo Horizonte, Minas Gerais, Brazil

M. J. B. Bezerra, T. M. Oliveira, G. A. Bezerra, and B. S. Cavada
Laboratório de Bioquímica Molecular, Departamento de Bioquímica, Universidade Federal do Ceará, Campus do Pici, 60455-900 Fortaleza, Ceará, Brazil

M. C. F. de Oliveira
Departamento de Química Orgânica e Inorgânica, Universidade Federal do Ceará, Campus do Pici, 60455-900 Fortaleza, Ceará, Brazil

M. Z. S. Flores, G. A. Farias, and V. N. Freire*
Departamento de Física, Universidade Federal do Ceará, Caixa Postal 6030, Campus do Pici, 60455-900 Fortaleza, Ceará, Brazil
(Received 23 June 2006; revised manuscript received 10 December 2006; published 21 March 2007)

Single crystals of monohydrated *L*-asparagine have been grown from aqueous solutions using $MnCl_2$ as doping material. Electron paramagnetic resonance (EPR) was used to determine the incorporation sites of Mn^{2+} ions in the crystal structure. Depending on small *p*H changes and crystal growth kinetics in the aqueous solutions, Mn^{2+} ions are incorporated in two chemically distinct sites in asparagine crystals. The first shows isotropic six-line hyperfine-split EPR spectra, whereas the second shows anisotropic multiple line splitting due to Mn^{2+} fine structure ($S=5/2$) and hyperfine interaction ($I=5/2$). Angular dependencies of the Mn^{2+} EPR spectra in three mutually perpendicular crystal planes were measured and analyzed. The results are discussed in terms of the metal incorporation site symmetry in the crystal structure of monohydrated *L*-asparagine.

DOI: 10.1103/PhysRevB.75.104205 PACS number(s): 71.20.Rv, 78.20.−e, 78.40.Me, 78.55.Kz

I. INTRODUCTION

About half of all proteins contains metal ions, which perform a wide variety of specific functions associated with life processes. In particular, transition metals such as Fe, Cu, and Mn are involved in many redox processes requiring electron transfer, and play an important role in the folding and biofunctionality of proteins, taking part of many enzymes and being indispensable in several catalytic reactions.[1] For example, the interaction between a tetranuclear Mn cluster and its protein ligand has a central role in photosystem II,[2] while the manganese ion in the vicinity of the saccharide-binding site in native Dguia lectin interacts with the asparagine residue Asn 14, contributing to the stabilization of the binding pocket.[3] The growth of amino acid crystals from aqueous solutions containing transition-metal ions allows us to study in the solid state the transition metal—amino acid interaction, helping to provide a solid foundation for the understanding of the role of transition metals in proteins.

To understand basic aspects of the role of metal in proteins, amino acid crystals doped with transition metals are appropriate model systems. Several works were published on different aspects of these crystals. Windsch and co-workers[4] investigated copper(II)-doped single crystals of glycine and triglycine sulfate, showing that each copper(II) ion is coordinated with two amino acid molecules. Takeda *et al.*[5] studied single crystals of copper(II)-doped *L*-alanine, demonstrating the existence of four chemically identical but magnetically nonequivalent sites through electron paramagnetic resonance (EPR) measurements. Winkler *et al.*[6] presented a study of low-concentration Fe(III) doping in crystalline *L*-alanine by means of EPR, Raman scattering, and photoluminescence, showing that Fe(III) occupies two inequivalent sites of rhombic symmetry in the *L*-alanine crystal. Other Fe(III)-related centers with isotropic EPR spectrum were mentioned; however, they were not analyzed. Calvo and co-workers[7–9] performed EPR studies of copper ion dopants in several amino acid crystals. For example, Dalosto *et al.*[7] performed EPR studies of copper ion dopants and Zn(*D*,*L*-histidine),[7] interpreting their experimental results with a model where the copper atoms hop randomly between different states, relating this dynamics to the fluctuating disorder in He lattices. Zeeman and hyperfine coupling tensors were determined for *L*-arginine phosphate monohydrate single crystals by Santana *et al.*,[8] who suggested that Cu impurities have three N ligands in this case. EPR was also used by Santana *et al.*[9] to study Cu(II) dopant ions in single crystals of bis(*L*-asparaginato)Zn(II), indicating that the Cu(II) impurities replace Zn(II) ions in the host crystal. Recently, Pinheiro *et al.*[10] performed EPR detection and first-principles calculations of manganese clusters in highly doped *L*-alanine crystals, demonstrating that manganese is incorporated into *L*-alanine crystals as Mn^{2+} ions at magnetically equivalent single interstitial sites in the unit cell for crystals grown with $MnCl_2$ concentrations smaller than 3.0% in the mother solutions, and at two or more neighboring interstitial sites in the case of higher $MnCl_2$ concentrations, which gives rise to manganese clusters in the doped *L*-alanine crystals. First-principles quantum mechanics and force field calculations suggested four interstitial sites for the manganese atoms in the *L*-alanine unit cell, and a high spin configuration (sextet with $S=5/2$) for the manganese electronic state.

Asparagine ($C_4N_2O_3H_8$) is one of the 20 natural amino acids, having an important role in the metabolic control of

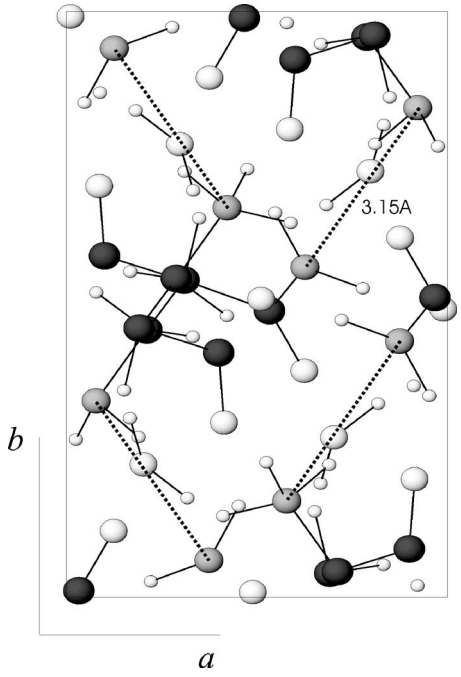

FIG. 1. Projection of the *L*-asparagine monohydrated structure on the ***ab*** plane. Atoms are nitrogen (gray), oxygen (white big), carbon (dark gray), and hydrogen (white small). The dashed lines indicate the distance of 3.15 Å between two nitrogen atoms.

some cell functions in nerve and brain tissues, playing important structural roles in proteins because their side-chain amide groups can act as both hydrogen bond acceptors and donors. In the solid state, the *L*-asparagine amino acid crystals are monohydrated, presenting orthorhombic structure, space group $P2_12_12_1$ (D_2^4), four molecules in the unit cell, and lattice parameters $a=5.593$ Å, $b=9.827$ Å, and $c=11.808$ Å.[11,12] Figure 1 shows the projection of the crystal structure on the ***ab*** plane. The asparagine molecules are in the zwitterionic state in monohydrated *L*-asparagine (MLASN) crystals, which are stabilized by several hydrogen bonds involving the water molecules, as demonstrated by infrared and Raman scattering studies of undoped MLASN crystals and deuterated derivatives.[13,14] Finally, three pressure-induced phase transitions in undoped MLASN crystals have been studied by Raman spectroscopy.[15]

The purpose of this work is to study how manganese is incorporated in monohydrated *L*-asparagine crystals. The focus is on EPR measurements and data analysis of Mn-doped single crystals of monohydrated *L*-asparagine. Angular dependencies of different samples were measured at room and low temperatures for three mutually perpendicular crystal planes. Two types of Mn^{2+}-related EPR spectra were observed: the first type shows isotropic six-line hyperfine-split EPR spectra that collapse to a broad line with some hyperfine structure for high doping levels, whereas the second type shows well-resolved anisotropic multiple EPR line spectra. Angular dependencies are calculated, taking into account electron Zeeman, hyperfine, and fine structure interactions due to the high electron spin $S=5/2$ and nuclear spin of $I=5/2$ of Mn^{2+} with 100% natural abundance. One magnetic site for Mn was observed with orientation of the magnetic field ***B*** along the crystal axes ***a***, ***b***, or ***c***, two inequivalent Mn sites occurs for ***B*** in the crystal planes ***ab***, ***bc***, or ***ac***, and four inequivalent sites were observed for arbitrary ***B*** directions, consistent with an orthorhombic crystal structure for Mn-doped MLASN crystal. The local site symmetry and the origin of the two types of Mn^{2+}-related EPR spectra are discussed.

II. CRYSTAL GROWTH AND EXPERIMENTAL SETUP

Manganese-doped MLASN crystals were grown by slow evaporation of aqueous *L*-asparagine solutions containing $MnCl_2$ concentrations form 0.5–7 % in mass. At least 50 different single crystals with well-formed natural faces and sizes of about $5\times3\times10$ mm^3 were obtained. The evaporation rate of the mother solutions and the existence of impurities and contaminants, which influence the tax of the growth of crystal planes, favor the incorporation of Mn^{2+} ions in chemically distinct sites in *L*-asparagine crystals. Very small dynamical variations in the *p*H of the mother solutions (due to the metal incorporation) and in the kinetic of growth are important factors that change the way the manganese ions are incorporated in the *L*-asparagine crystals, allowing different sites for incorporation. For the EPR measurements, samples were cut to pieces of about $3\times3\times3$ mm^3 taking advantage of the well-formed crystal faces for orientation of the samples. EPR spectra were recorded on a homemade heterodyn spectrometer with a 500 mW klystron (Varian), a commercial cylindrical resonance cavity (Bruker), an electromagnet (Varian) with maximum field amplitudes of 800 mT, and a He flux cryosystem (Oxford) for low-temperature measurements. For the angular variations, the sample holder was rotated with a goniometer in steps of 5° with a precision of about 0.2°. Microwave frequency was stabilized by an automatic frequency control and measured with high precision frequency meter (PTS). For *g*-factor calibration, the 2,2-Diphenyl-1-pikryl-hydrazil (DPPH) standard has been used ($g=2.0037$). Spectra were recorded as first derivates using common 100 kHz field modulation and lock-in technique (EG & G Princeton).

III. EXPERIMENTAL RESULTS

EPR measurements were performed in the as-grown 50 manganese-doped asparagine crystals, showing the existence of two different types of metal incorporation that give rise to two distinct EPR features. Three EPR spectra are shown in Fig. 2, [(a) and (b)] resulting from measurements at room temperature on typical *L*-asparagine crystals with manganese incorporated in two different sites, and (c) depicting a simulated EPR spectrum with the parameters shown in Table I. For one set of samples, the EPR spectra are isotropic with respect to crystal and magnetic field orientations since Fig. 2(a) reveals a six-line hyperfine split EPR spectrum, typical for Mn^{2+} with very weak fine structure interaction (Mn^{2+} has electronic spin $S=5/2$ and $I=5/2$ with 100% natural abundance). On the other hand, Fig 2(b) shows a multiple fine structure and hyperfine structure split anisotropic EPR spectrum of Mn^{2+} ions in intermediate crystal fields.[15] It consists

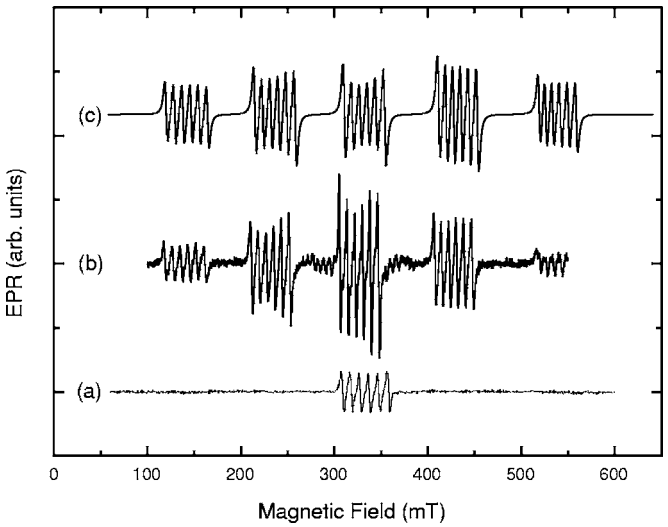

FIG. 2. EPR spectra measured at room temperature in two different *L*-asparagine monocyrstals: (a) isotropic six-line hyperfine split spectrum of Mn^{2+}, (b) multiple line spectrum of Mn^{2+} split by the electronic fine structure and hyperfine interaction of Mn^{2+}, and (c) calculated EPR spectrum for situation (b).

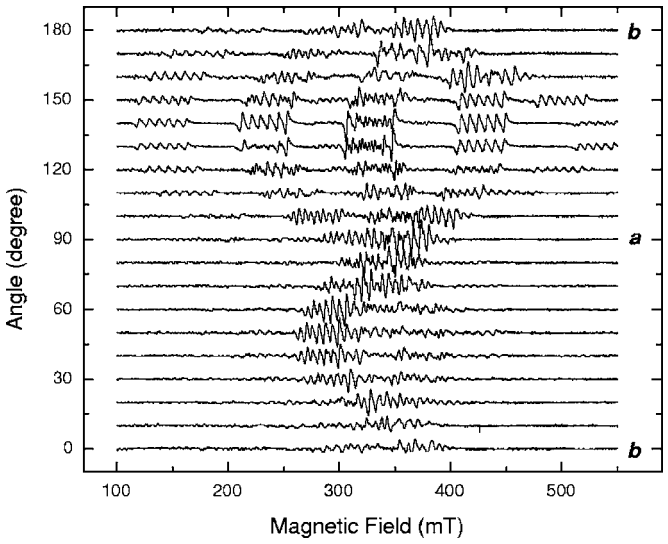

FIG. 3. EPR angular dependence of a monohydrated *L*-asparagine monocrystal doped with Mn^{2+} measured at room temperature. The magnetic field is applied in the ***ab*** plane, and **c** is the rotation axis.

of five packets due to electronic fine structure interaction split into six lines by the central hyperfine interaction.

EPR angular dependencies were measured in three mutually perpendicular crystal planes. The EPR spectra and angular dependencies are complicated due to the multiple line superposition. Figure 3 shows the rotational pattern of the EPR spectra of the anisotropic Mn^{2+} spectrum in the ***ab*** plane with perpendicular rotation axis along ***c***. The Mn^{2+}-related EPR spectra are characterized by two magnetically inequivalent sites for rotation in the crystal planes ***ab***, ***ac***, and ***bc***. In case of misalignment of samples, the two inequivalent sites spectra are further split into four inequivalent sites. It is interesting to note that the intensity of EPR lines due to the two inequivalent sites is not equally distributed, presenting an intensity ratio of about 5:1. Similar intensity ratios were also observed for Cu^{2+}-doped L-alanine samples,[16] which was explained as due to the *g* factor anisotropy they had measured. It was found that the site distribution is strongly dependent on concentration of the dopant ions. At low concentrations, the copper ions populate both sites equally, whereas for higher concentrations one site is preferred because of mutual interactions between the dopant ions. A small distortion may be induced lowering the energy of one of the both sites. In Sec. IV, we present data on the *g* factor anisotropy in our Mn^{2+}-doped asparagine crystals explaining the different intensities.[16,17]

TABLE I. Parameters for the Mn^{2+} spin Hamiltonian in monohydrated *L*-asparagine. *g* is the Zeeman interaction and *D* the fine structure interaction (GHz).

	g_{xx}	g_{yy}	g_{zz}
	2.025(5)	2.017(5)	1.992(5)
θ	47°	113°	128°
φ	105°	39°	148°
	D_{xx}	D_{yy}	D_{zz}
	0.95(1)	0.02(1)	−0.97(1)
θ	94°	56°	146°
φ	44°	316°	309°

The EPR angular dependencies are dominated by the electron Zeeman and fine structure interaction due to the Mn^{2+} electronic spin $S=5/2$. Since hyperfine interaction due to the interaction with the Mn^{2+} nuclear spin $I=5/2$ is small, it is omitted in the first analysis. Figure 4 shows the EPR angular dependence in the ***ab*** plane, in which the line positions were determined from the center position of each of the five electronic fine structure line packets (shown as dots).

IV. DISCUSSION

The EPR spectra and angular dependencies of the Mn^{2+} centers are analyzed using the following spin Hamiltonian in orthorhombic symmetry:

$$H = \beta \mathbf{S} g \mathbf{B} + \mathbf{S} D \mathbf{S} + \mathbf{S} A \mathbf{I} + \sum_{m=0,\pm 2,\pm 4} B_4^m O_4^m. \qquad (1)$$

The first term in Eq. (1) represents the electronic Zeeman interaction, the second the electronic fine structure interaction, the third the hyperfine interaction, and the fourth term is due to fourth order terms in Stevens notation.[17] The parameters of Eq. (1) have their usual meaning.[17]

The parameters of the spin Hamiltonian of the anisotropic Mn^{2+}-related EPR spectra were evaluated by fitting simultaneously all line positions in the three mutually perpendicular crystal planes (shown in Figs. 3 and 4 for the ***ab*** plane) using exact diagonalization of the spin Hamiltonian of Eq. (1) for the orthorhombic symmetry and omitting hyperfine interaction. In the analysis, 256 line positions were taken into ac-

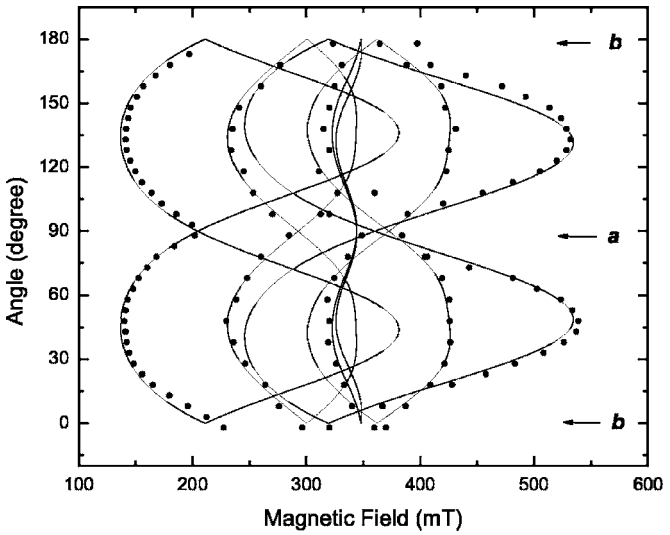

FIG. 4. Rotational pattern of EPR angular dependencies in the ***ab*** plane. The dots correspond to the center line positions and the solid lines to the calculated pattern.

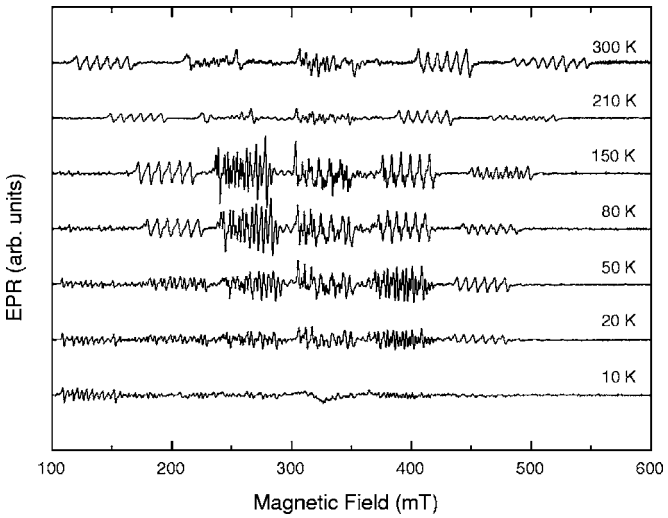

FIG. 5. Temperature dependence of the EPR spectra for orientation of the magnetic field near the diagonal of the ***ab*** plane of a monohydrated *L*-asparagine crystal.

count. The anisotropy of the EPR spectrum is dominated by the electronic fine structure. The line positions with large fine structure splitting are more weighted than lines in regions of multiple superpositions. Parameters from the fitting routines are shown in Table I. From the analysis, it is found that the g tensor has orthorhombic symmetry with only a small anisotropy, and that the axial and rhombic parts of the electronic fine structure tensor, D and E, have different signs. In the principal axis system of the fine structure tensor D, the parameters are determined: $|D|=1.47(1)$ GHz and $|E|=0.467(5)$ GHz, with a high $\sim E/D=-0.32$ asymmetry ratio. The principal axis lies nearly in the diagonal of the ***ab*** plane perpendicular to the ***c*** axis. The inclusion of the fourth degree Stevens parameters, the fourth term in Eq. (1), decreases only the total error weakly in the adjusted line positions.

The EPR absorption intensity depends generally on the g *anisotropy*. The theory is well established and described in standard references.[17] The EPR intensity for an allowed transition is proportional to the intensity factor g_1, which is related to $\boldsymbol{g}$ through its principal values and the direction cosines of the vector $\boldsymbol{u}\times\boldsymbol{u}_1$, where $\boldsymbol{u}$ and $\boldsymbol{u}_1$ are the unit vectors along the applied static and oscillating magnetic fields, respectively.[16,17] The expression for the intensity factor (and consequently the EPR absorption) g_1 depends on the principal $\boldsymbol{g}$ values and the angle between the static field and the principal axis, in such a way that the intensity ratio between two directions presents a fourth power dependence on the reason between g_x, g_y, and g_z, the principal g values. Consequently, the g *anisotropy* explains the intensity ratio of about 5:1 we have presented in Fig. 3. As already mentioned before, similar intensity ratios were also observed for Cu^{2+}-doped *L*-alanine samples,[16] which was one of the first particular evidence that the EPR absorption intensity is related directly to the g anisotropy.

The absolute sign of the parameters of the fine structure tensor is determined from the temperature dependence of the EPR spectra along the principal direction of the tensor. Figure 5 shows the temperature dependence of the Mn^{2+}-related EPR spectra for orientation of the magnetic field near the diagonal of the ***ab*** plane. From Fig. 5, it can be observed that the high field line packet increases in intensity when the temperature is lower, contrary to the low field line packet. This means that D is negative.[13] At very low temperatures, the EPR spectra start to saturate. The EPR angular dependencies measured at 50 K indicate a strong reduction in the amplitude of the fine structure parameters and also of the asymmetry parameter. However, the point symmetry of the Mn^{2+} site is basically the same. D and E are reduced at 50 K to -1.20 and 0.26 GHz, respectively, producing an asymmetry ratio $E/D=0.22$.

The hyperfine interaction of Mn^{2+}, which has nuclear spin $I=5/2$, could not be analyzed in detail because of several line superpositions due to the two magnetically inequivalent sites, as well as misalignment effects. However, from the spectra some estimates were done. The hyperfine interaction is strongly anisotropic varying from 5.5(5) to 9.5(5) mT with the principal tensor axis nearly along ***c***, perpendicular to the fine structure tensor axis. Such hyperfine values are expected for octahedral rather than tetrahedral coordination.[17]

Nitrogen superhyperfine interaction is mostly hidden in the linewidth of the Mn^{2+} hyperfine lines with individual line width $\Delta B_{pp}\approx 1.4$ mT. However, for some orientations, nitrogen superhyperfine interaction is poorly resolved, indicating at least interaction from two nitrogen neighbors. If we take into account also the D tensor orientation, then we conclude that Mn^{2+} ions are located between two amino groups, which belong to two different molecule distantances of 3.15 Å, as shown in Fig. 1. Such geometry also implies that two nearest carboxyl groups from the same two asparagine molecules are close to the Mn^{2+} ions. The two nitrogen atoms bounded to the Mn^{2+} ions are situated nearly in the diagonal of the ***ab*** plane, more precisely making angles of 58° and 32° with the ***a*** and ***b*** axes, respectively. A small rearrangement may occur when Mn^{2+} enters between them. To determine the exact symmetry position, electron nuclear double resonance mea-

surements of the nitrogen superhyperfine interaction is required. A similar bonding site was also suggested for Cu^{2+} ions in dimetylalanine and α-glycine,[18] somewhat different for the case of Cu^{2+} incorporation in *L*-alanine, which is bound to three alanine, molecules.[5] The EPR analysis of Fe^{3+} in *L*-alanine by Winkler *et al.*[6] should be taken with care because the fine structure parameters of Fe^{3+} were not determined. An isotropic Fe^{3+}-related EPR spectrum was reported; however, it was not analyzed.

The isotropic six-line hyperfine-split EPR spectrum of Mn^{2+} ions in monohydrated *L*-asparagine is described by an isotropic *g* factor of 2.002(1) and hyperfine interaction of 9.8(2) mT, taking into account the first and third terms of Eq. (1). The individual EPR line width $\Delta B_{pp} \sim 3.5$ mT is explained by unresolved superhyperfine interactions. The isotropic Mn^{2+} EPR spectrum in some of the samples is attributed to a variation of the *p*H and the velocity of crystal growth. In this case, Mn^{2+} can either be included in the asparagine structure near the water molecules with no well-defined symmetry site or incorporated as liquid or solid inclusions. The first possibility is discarded because at the lowest measurement temperatures (about 10 K), the EPR spectrum is still isotropic. One should imagine that at least at low temperatures, a special configuration site would be frozen in, while the site symmetry is not well defined at higher temperature due to rotation of the water molecules in the structure, causing some disorder.

As in the well known case of the growth of protein crystals, there are many factors that give rise to the growth of amino acid crystals as a subtle phase transition. The purity of the water and reagents, the temperature of the ambient and of the water bath, the evaporation rate of the mother solutions, the flux of mother solution in the beackers, the dynamical small changes of the *p*H of the mother solutions during the growth process (principally due to the metal incorporation), and contaminations are the factors that can change the way manganese is incorporated in asparagine crystals. In particular, impurities and contamination of the order or below 1% (which are difficult to control) can favor planes of growth of the crystals and, consequently, the sites for metal incorporation. Further studies on the growth parameters are still necessary in order to distinguish what kind of growth parameters has the main influence on the type of manganese incorporation site.

V. SUMMARY

The detailed analysis of the Mn^{2+} EPR spectra in doped monohydrated *L*-asparagine monocrystals allow us to conclude that Mn^{2+} ions enter in two chemically nonequivalent positions in interstitial sites. The first is related to the isotropic EPR spectra with suppressed fine structure interaction. This site is only loosely bound to water molecules or manganese enters as solid or liquid inclusions during growth. The anisotropic Mn^{2+}-related center is more strongly bound to the crystal lattice maintaining the orthorhombic crystal symmetry. It shows intermediate zero-field splitting with strong asymmetry ratio E/D of -0.32 and -0.22 at 300 and 50 K, respectively. The incorporation site of Mn^{2+} occurs between two amino and two carboxyl groups belonging to two different asparagine molecules.

ACKNOWLEDGMENTS

K.K., B.S.C., and V.N.F. are senior researchers of the Conselho Nacional de Pesquisa Científica e Desenvolvimento Tecnológico (CNPq) in Brazil. B.S.C. and V.N.F. received financial support from project CNPq-Rede Nano-Bioestruturas, No. 555183/2005-0. K.K. acknowledges financial support from the Brazilian agencies FAPEMIG, FINEP, CNPq, and CAPES. T.M.O., G.A.B., and M.Z.S.F. received support from CNPq during the development of this work.

*Corresponding author. Email address: valder@fisica.ufc.br

[1] T. Dudev and C. Lim, Chem. Rev. (Washington, D.C.) **103**, 773 (2003).
[2] N. Mizusawa, T. Tamanari, Y. Kimura, A. Ishii, S. Nakazawa, and T. Ono, Biochemistry **43**, 15644 (2004).
[3] D. A. Wah, A. Romero, F. G. del Sol, B. S. Cavada, M. V. Ramos, T. B. Grangeiro, A. H. Sampaio, and J. J. Calvete, J. Mol. Biol. **310**, 885 (2001).
[4] A. Lösche and W. Windsch, Phys. Status Solidi **11**, K55 (1965); M. Welter and W. Windsch, Wiss. Z.-Karl-Marx-Univ. Leipzig, Math.-Naturwiss. Reihe **15**, 309 (1966); W. Windsch and M. Welter, Z. Naturforsch. A **22A**, 1 (1967).
[5] K. Takeda, Y. Arata, and S. Fuyiwara, J. Chem. Phys. **53**, 854 (1970).
[6] E. Winkler, A. Fainstein, P. Etchegoin, and C. Fainstein, Phys. Rev. B **59**, 1255 (1999).
[7] S. D. Dalosto, R. Calvo, J. L. Pizarro, and M. I. Arriortua, J. Phys. Chem. A **105**, 1074 (2001).
[8] R. C. Santana, J. F. Carvalho, S. R. Amaral, I. Vencatto, F. Pelegrini, M. C. Terrile, A. C. Hernandes, and R. Calvo, J. Phys. Chem. Solids **63**, 1857 (2002).
[9] R. C. Santana, M. G. Santos, R. O. Cunha, K. D. Ferreira, J. F. Carvalho, and R. Calvo, J. Phys. Chem. Solids **67**, 745 (2006).
[10] J. R. Pinheiro, E. W. S. Caetano, V. N. Freire, G. A. Farias, K. Krambrock, M. C. F. de Oliveira, J. A. Pinheiro, B. S. Cavada, and J. L. de Lima Filho, Appl. Phys. Lett. (submitted).
[11] J. L. Wang, Z. Berkovitch-Yellin, and L. Leiserowitz, Acta Crystallogr., Sect. B: Struct. Sci. **B41**, 341 (1985).
[12] W. D. Arnold, L. K. Sanders, M. T. McMahon, A. V. Volkov, G. Wu, P. Coppens, S. R. Wilson, N. Godbout, and E. Oldfield, J. Am. Chem. Soc. **122**, 4708 (2000).
[13] J. Casado, J. T. López Navarrete, and F. J. Ramírez, J. Raman Spectrosc. **26**, 1003 (1995).
[14] J. Casado, J. T. López Navarrete, and F. J. Ramírez, J. Mol. Struct. **349**, 57 (1995).
[15] A. J. D. Moreno, P. T. C. Freire, F. E. A. Melo, M. A. Araújo Silva, I. Guedes, and J. Mendes Filho, Solid State Commun. **103**, 655 (1997).
[16] M. Fujimoto and Y. Tomkiewicz, J. Chem. Phys. **56**, 749 (1972).
[17] A. Abragam and B. Bleaney, *Electron Paramagnetic Resonance of Transition Ions* (Dover, New York, 1986).
[18] K. Takeda, Y. Arata, and S. Fujiwara, J. Chem. Phys. **55**, 1152 (1971).